Improvement of Pattern Null Depth and Width Using a Curved Array With Two Subarrays for CRPA Systems

Gangil Byun, Hosung Choo, and Sunwoo Kim

***Abstract*—This communication proposes a curved array split into two subarrays to improve the pattern null depth and width for controlled reception pattern antenna (CRPA) systems. The proposed array consists of a single reference element at the center and two subarrays that are arranged on a spherical coverture. To consider both signal processing and electromagnetic (EM) perspectives, array patterns are calculated by using a microstrip patch antenna in conjunction with a constraint least-mean-square (LMS) algorithm. The proposed array shows significant improvement in the pattern null depth and width compared to a uniformly distributed circular array.**

***Index Terms*—Adaptive antenna array, antenna array, CRPA array, GPS antenna, null steering array.**

I. Introduction

A controlled reception pattern antenna (CRPA) array is widely used for a global positioning system (GPS) to suppress interference by steering pattern nulls toward interference sources. In this null steering operation, array weights are updated in accordance with a space-time adaptive processing (STAP) algorithm that minimizes the output power of the array. Since the array should be capable of tracking GPS satellites in both azimuth and elevation, a uniform circular array (UCA) has been a suitable configuration in many applications. However, the planar arrangement of the UCA results in a low signal-to-interference-plus-noise ratio (SINR) at low elevations because of its poor null steering performance. For this reason, many adaptive algorithms have been developed to improve the SINR by determining the optimum array weights from a signal processing perspective, as in [1]−[4]. Much effort has also been made by applying various design approaches for individual array elements to improve their radiation characteristics from an electromagnetic (EM) perspective [5]–[8]. These two perspectives have been combined in [9]; however, this communication is mainly focused on how the spherical curvature of the array affects the SINR performance, and there has not yet been an in-depth analysis on array patterns to improve the null steering performance.

In this communication, the null steering performance is improved by splitting the CRPA array into two subarrays arranged on a spherical curvature. The proposed array is composed of a single reference element and two subarrays having eight auxiliary elements, and its configuration is adjusted by element positions, array radius, and the array curvature. The first subarray is designed to have more antenna elements compared with the second subarray to minimize the null steering ambiguity for all azimuth angles, and the second array is designed to have a larger aperture size for maximizing the null steering resolution. To consider both signal processing and EM perspectives, we calculate the array pattern using a microstrip patch antenna, as proposed in [10], in conjunction with a constrained least-mean-square (LMS) algorithm, as presented in [11]. The suitability of the proposed array is evaluated by comparing its null steering performance with an eight-element UCA with a center reference element. The results demonstrate that the proposed array improves the null steering performance by forming deeper and sharper nulls, even for low-elevation interference sources.

Manuscript received August 14, 2014; revised December 26, 2014; accepted March 21, 2015. Date of publication March 27, 2015; date of current version May 29, 2015. This work was supported by the Civil Military Cooperation (CMTC) and Basic Science Research Program through the National Research Foundation of Korea (NRK) funded by the Ministry of Education (NRF-2014R1A1A2055813).

G. Byun and S. Kim are with the Department of Electronics and Computer Engineering, Hanyang University, Seoul 133-791, Korea (e-mail: remero@hanyang.ac.kr).

H. Choo is with the School of Electronic and Electrical Engineering, Hongik University, Seoul 121-791, Korea.

Digital Object Identifier 10.1109/TAP.2015.2416758

II. Proposed Array Configuration

A. Design Parameters

Fig. 1 shows the design parameters of the proposed array having nine identical antennas whose reflection coefficient is $-13.1\,\mathrm{dB}$ with bore-sight gain of $-0.5\,\mathrm{dBic}$ and a half power beam width of 92° [9]. The array consists of a single reference element at the top of a sphere with a radius of r_s and eight auxiliary elements that are arranged in two circular subarrays. The radii of the two subarrays are denoted as r_1 and r_2 and are defined in (1). The heights of the subarrays are expressed as h_1 and h_2, and their definitions are shown in (2). These values are varied by adjusting values of θ_1 and θ_2, which are also used to define the surface curvature of the array, as shown in (3).

$$\begin{cases} r_1 = r_s \sin\theta_1 \\ r_2 = r_s \sin\left(\theta_1 + \theta_2\right) \end{cases} \tag{1}$$

$$\begin{cases} h_1 = r_s \left(1 - \cos\theta_1\right) \\ h_2 = r_s \left(1 - \cos\left(\theta_1 + \theta_2\right)\right) \end{cases} \tag{2}$$

$$k = \frac{\theta_1 + \theta_2}{r_2} \tag{3}$$

In addition, the angular positions of the auxiliary elements are determined by the parameters of ϕ_1, $\phi_2, \ldots,$ and ϕ_8, as illustrated in Fig. 1(b). Fig. 2 shows an eight-element UCA with a center reference element that has been commonly used in many CRPA applications because of its wide pattern scanning range in both azimuth and elevation. The null steering performance of this UCA configuration is compared to that of the proposed configuration in conjunction with a CRPA system whose detailed descriptions are specified in the following chapter.

B. Implementation of a CRPA System

To estimate the null steering performance, we built a CRPA system using the constraint LMS algorithm proposed in [10]. The algorithm iteratively updates array weights to minimize the output power of the array without a *priori* knowledge of the interference direction. It is assumed that 10 GPS L1 satellites exist in the upper hemisphere, whose positions were obtained from a commercial GPS receiver placed on a rooftop of a building ($\mathrm{height} = 13\,\mathrm{m}$, Pangyo, Korea) in clear weather (temperature: $27.5^\circ\mathrm{C}$, humidity: 62.6%), and their average power incident to the array aperture is about $-130\,\mathrm{dBm}$ [12]. In addition, the noise floor of the system is $-104.5\,\mathrm{dBm}$, which implies that the signal-to-noise ratio (SNR) is about $-20\,\mathrm{dB}$ with an antenna gain of 5 dBic. It is also assumed that an independent interference signal arrives at an elevation angle (θ_{EL}) of 15° for all azimuth directions, and its peak power is $-50\,\mathrm{dBm}$ over the frequency range from 1.45 to 1.65 GHz. This interference signal is then suppressed by the null steering process to calculate the pattern null depth and width, which are defined as follows:

$$\mathrm{Cost}\ 1 = \left|G_{fin}\left(\theta,\phi\right) - G_{ini}\left(\theta,\phi\right)\right| \tag{4}$$

$$\mathrm{Cost}\ 2 = \left|\Omega_{upper} - \Omega_{lower}\right|_{G_{fin}=-20\ \mathrm{dBic}} \tag{5}$$

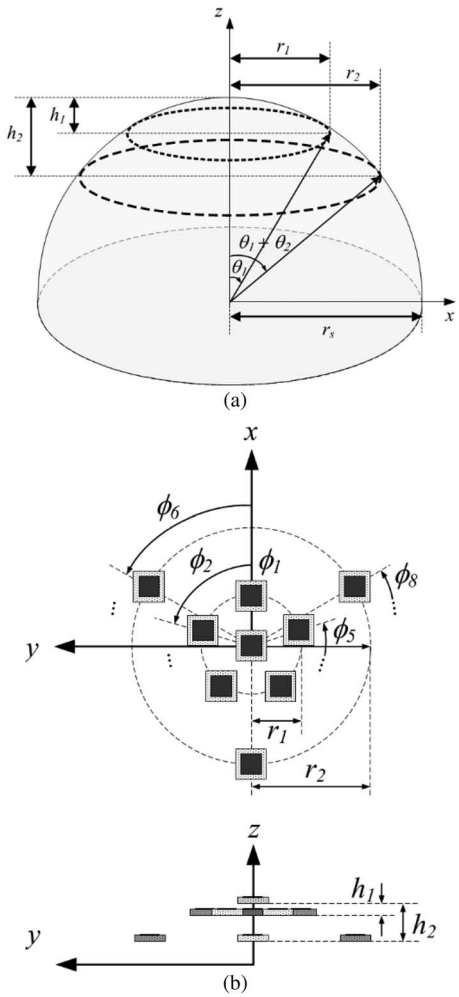

Fig. 1. Proposed array configuration. (a) Design parameters. (b) Antenna arrangement.

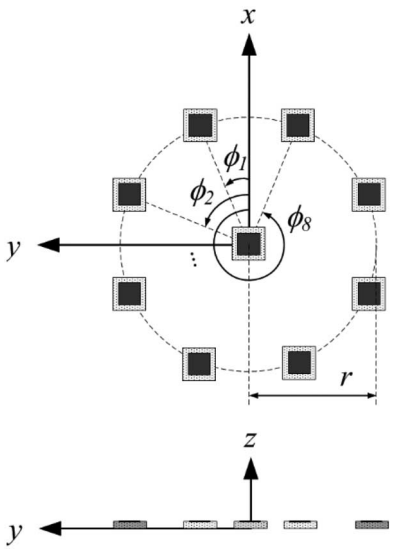

Fig. 2. UCA configuration.

where G_{ini} indicates the initial array gain value in dBic at each interference direction before the adaptive process, and G_{fin} denotes the final array gain value in the same direction after the null steering process. The null width is defined as the angular difference

TABLE I
PARAMETERS OF ARRAY CONFIGURATIONS

Parameters	UCA configuration	Proposed array configuration
Number of antennas	9	9
Curvature (k)	0	5.3
r	97.3 mm ($0.51\lambda_0$)	–
r_1	–	41.3 mm ($0.22\lambda_0$)
r_2	–	97.3 mm ($0.51\lambda_0$)
h_1	–	4.4 mm ($0.02\lambda_0$)
h_2	–	25.7 mm ($0.14\lambda_0$)
ϕ_1	22.5°	0°
ϕ_2	67.5°	72°
ϕ_3	112.5°	144°
ϕ_4	157.5°	216°
ϕ_5	202.5°	288°
ϕ_6	247.5°	60°
ϕ_7	292.5°	180°
ϕ_8	337.5°	300°

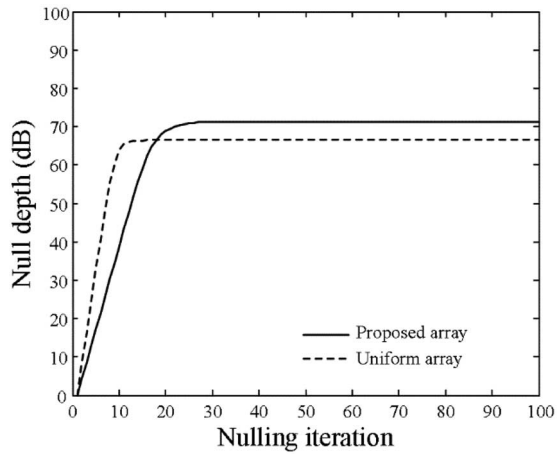

Fig. 3. Null depth variation according to LMS nulling iterations.

between two points (Ω_{upper}, Ω_{lower}) of a null steering pattern satisfying $G_{fin} = -20\,\text{dBic}$, which was determined by considering the processing gain of the system. The pattern null depth and width are evaluated for independently located interference sources at $\phi = 0°$, $30°, \ldots,$ and $330°$, and their average values are used for cost functions to find the optimum element positions, array radius, and curvature using a genetic algorithm (GA), as introduced in [13]. Table I shows the optimized design parameters of the proposed array in comparison with the UCA configuration. Since the cost values were averaged for all interference directions, evenly distributed arrays were obtained after a large number of GA iterations. In addition, the second subarray of the proposed configuration was optimized to be more than twice as large as the first subarray, and the two subarrays were arranged on a curved surface with the curvature of 5.3. This curvature allows the array to have a height difference of $h_2 = 25.7\,\text{mm}$ between the center

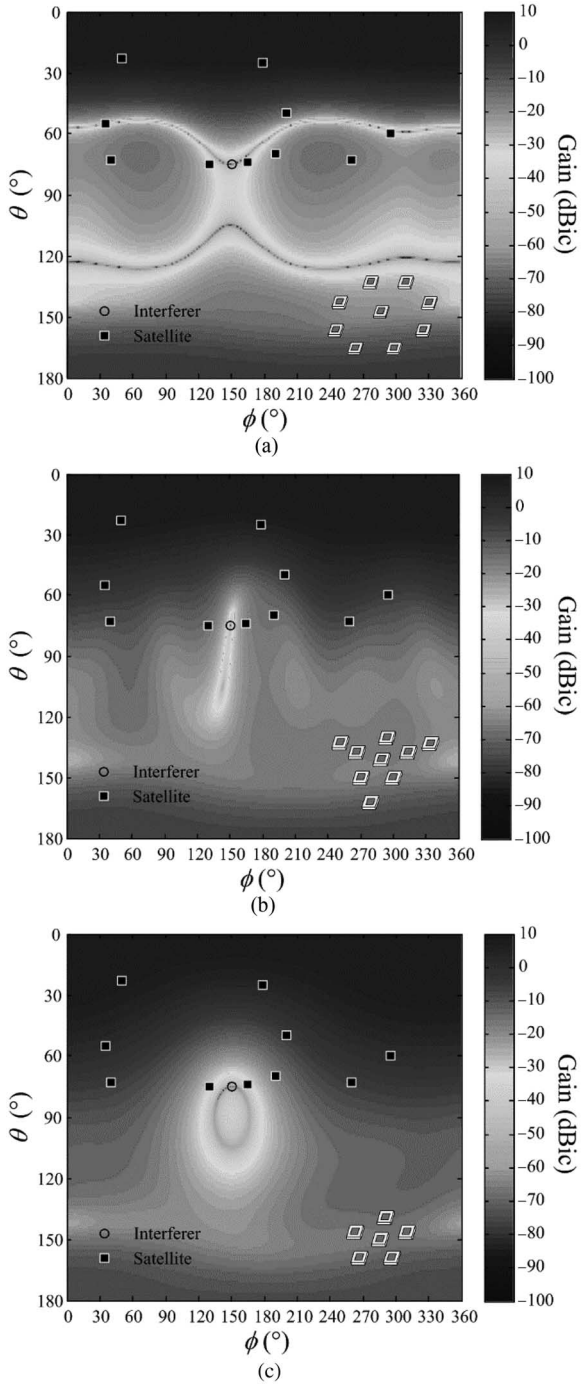

Fig. 4. Comparison of array patterns after null steering. (a) UCA configuration. (b) Proposed array configuration. (c) Proposed array configuration with no second array.

reference element and the second subarray, which improves the null steering resolution at low elevation angles. To verify the suitability of this configuration, it was compared to a UCA having the same number of elements and the same aperture size in the next section.

III. Performance Evaluation

Fig. 3 shows a variation in the pattern null depth according to the LMS iteration at $\theta_{EL} = 15^\circ$. The average null depth of the proposed array, presented by a solid line, is about 71.2 dB and is improved by

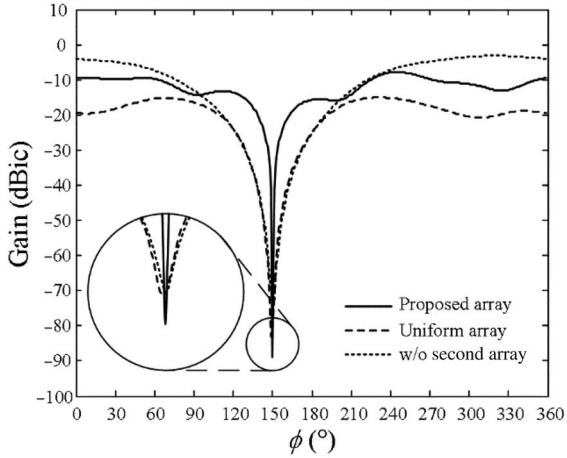

Fig. 5. Comparison of array pattern nulls.

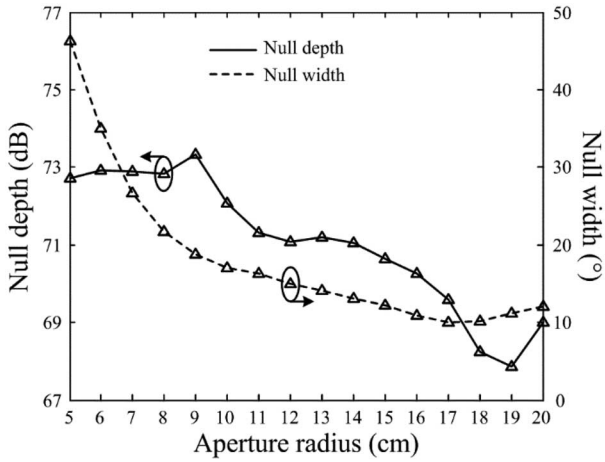

Fig. 6. Variations in the null depth and width according to aperture radius.

4.8 dB compared to the UCA configuration as denoted by a dashed line. The proposed array was further evaluated by varying the elevation angle of interference sources from $\theta_{EL} = 0^\circ$ to $\theta_{EL} = 30^\circ$, and it was verified that the array shows consistently deeper null depths compared to the UCA configuration. Fig. 4 presents a comparison of array patterns after the null steering process when an interference source is located at $\phi = 150^\circ$ and $\theta_{EL} = 15^\circ$. The source position is specified by a circle, and the satellite positions are shown as square markers. As can be seen in Fig. 4(a), the UCA configuration forms an undesired null at around $\theta = 60^\circ$ that lowers the power of satellite signals at lower elevations. On the other hand, the proposed array forms a much sharper null compared to the UCA configuration and barely affects the array patterns in the directions of the satellites. Fig. 4(c) shows a null steering pattern of the proposed configuration without the second array. It is provided to explain that the sharper null width was achieved by adding the second array with the larger aperture size. A significant improvement can also be found in Fig. 5 that compares azimuth patterns at $\theta_{EL} = 15^\circ$. The proposed configuration shows that the final array gain in the direction of the interference source is improved by 7.9 dB compared to the UCA configuration, and the pattern null width is also improved from 83.0° to 24.4° by adding the second array as discussed in Fig. 4.

The proposed array configuration is further evaluated by observing the variations in the pattern null depth and width according to its aperture radius, as shown in Fig. 6. In this evaluation, the curvature is fixed

at 5.3, and the values of θ_1 and θ_2 are adjusted in relation to (3). The results show that the pattern null width is reduced by the increased aperture radius; however, the pattern null depth tends to be increased as the aperture size becomes larger. Thus, the optimum aperture radius can be found within the range 9–10 cm, which includes the optimum array radius of the proposed array configuration.

IV. Conclusion

We have investigated the curved array split into two subarrays to improve the null steering performance for CRPA systems. The proposed array is composed of a single reference element at the center and two subarrays that are placed on the spherical curvature. Both signal processing and EM perspectives were taken into account by calculating array patterns using a microstrip patch antenna in conjunction with the constraint LMS algorithm. The optimum element positions, array radius, and array curvature were found by optimizing the pattern null depth and width, and the suitability of the proposed array was evaluated by comparing its null steering performance with the UCA configuration. The results demonstrated that the pattern null depth and width of the proposed array were improved by 4.8 dB and 58.6°, respectively, for low-elevation interference sources.

References

[1] M. Li, A. G. Dempster, A. T. Balaei, C. Rizos, and F. Wang, "Switchable beam steering/null steering algorithm for CW interference mitigation in GPS C/A code receivers," *IEEE Trans. Aerosp. Electron. Syst.*, vol. 47, no. 3, pp. 1564–1579, Jul. 2011.

[2] S. T. Smith, "Optimum phase-only adaptive nulling," *IEEE Trans. Signal Process.*, vol. 47, no. 7, pp. 1835–1843, Jul. 1999.

[3] R. L. Haupt, "Phase-only adaptive nulling with a genetic algorithm," *IEEE Trans. Antennas Propag.*, vol. 45, no. 6, pp. 1009–1015, Jun. 1997.

[4] C. C. Ko, "A fast adaptive null-steering algorithm on output power measurements," *IEEE Trans. Aerosp. Electron. Syst.*, vol. 29, no. 3, pp. 717–725, Jul. 1993.

[5] M. Chen and C.-C. Chen, "A compact dual-band GPS antenna design," *IEEE Antennas Wireless Propag. Lett.*, vol. 12, pp. 245–248, Feb. 2013.

[6] R. O. Ouedraogo, E. J. Rothwell, A. R. Diaz, K. Fuchi, and A. Theme, "Miniaturization of patch antennas using a metamaterial-inspired technique," *IEEE Trans. Antennas Propag.*, vol. 60, no. 5, pp. 2175–2182, May 2012.

[7] Y. Zhou, C.-C. Chen, and J. L. Volakis, "Single-fed circularly polarized antenna element with reduced coupling for GPS arrays," *IEEE Trans. Antennas Propag.*, vol. 56, no. 5, pp. 1469–1472, May 2008.

[8] S. X. Ta, J. J. Han, and I. Park, "Compact circularly polarized composite cavity-backed crossed dipole for GPS applications," *J. Electromagn. Eng. Sci.*, vol. 13, no. 1, pp. 44–50, Mar. 2013.

[9] J. R. Lambert, C. A. Balanis, and D. DeCarlo, "Spherical cap adaptive antennas for GPS," *IEEE Trans. Antennas Propag.*, vol. 57, no. 2, pp. 406–413, Feb. 2009.

[10] G. Byun, S. Kim, and H. Choo, "Design of a dual-band GPS antenna using a coupled feeding structure for high isolation in a small array," *Microw. Opt. Tech. Lett.*, vol. 56, no. 2, pp. 359–361, Feb. 2014.

[11] O. L. Frost, III, "An algorithm for linearly constrained adaptive array processing," *Proc. IEEE*, vol. 60, no. 8, pp. 926–935, Aug. 1972.

[12] K. Borre, D. M. Akos, N. Bertelsen, P. Rinder, and S. H. Jensen, *A Software-Defined GPS and Galileo Receiver*. Boston, MA, USA: Bitkhauser, 2007.

[13] G. Byun, H. Choo, and H. Ling, "Optimum placement of DF antenna elements for accurate DOA estimation in a harsh platform environment," *IEEE Trans. Antennas Propag.*, vol. 61, no. 9, pp. 4783–4791, Sep. 2013.

A Simple Transformation for Near-Singular Integrals on Curvilinear Elements

Haobo Yuan, Zhijun Wang, Xiaojie Dang, and Nan Wang

***Abstract*—It is difficult to evaluate the near-singular four-dimensional integrals in the Galerkin magnetic-field integral equations (MFIE), especially for the curvilinear elements. This communication presents a hyperbolic transformation to cancel the near singularities in the $1/R^2$ kernel on curved quadrilateral elements, which is addressed theoretically and numerically. This method has a much simpler formula than the so-called DIRECTFN method, and its convergence rate may be much faster than the latter. This is demonstrated by evaluating the near-singular integral of a sharp-edged structure composed of two curvilinear quadrilaterals.**

***Index Terms*—Curvilinear quadrilateral, magnetic-field integral equation (MFIE), near singularity, transformation.**

I. Introduction

An accurate and efficient integration of a $1/R^2$ near-singular kernel on curved surface is the prerequisite for the higher order moment method [1], [2] solution to the magnetic-field integral equation (MFIE). A number of schemes have been developed to handle the near singularity on flat triangle elements [3]–[12], whereas the literature about the near singularity on curved triangles or curved quadrilaterals is scarce [13], [14]. Obviously, the schemes for curved elements are much more difficult than that for flat elements, and the former is not a ready extension of the latter.

The impedance of the MFIE formulation is a four-dimensional integral composed of an inner surface integral over the source element and an outer surface integral over the observation element. When the source element coincides with the observation element, there is a $1/R$ singularity in the integrand of the inner surface integral, which is often handled by singularity subtraction methods for flat triangle elements [3], [14], or variable transformations for curved elements [15]–[17]. Although these transformations are suitable for the singularity when the observation point is right on the source element, they are not suitable for the near singularity when the observation point is just very close to the source element. This near singularity arises when the source element shares a common edge with the observation element. There is not only a $1/R^2$ near singularity in the integrand of the inner surface integral, but also a weak logarithmic singularity in the integrand of the outer surface integral [5].

Manuscript received May 22, 2014; revised February 03, 2015; accepted February 20, 2015. Date of publication March 30, 2015; date of current version May 29, 2015. This work was supported in part by the National Natural Science Foundation of China under Grant 61072018 and Grant 60901030, in part by the China Postdoctoral Science Foundation under Grant 2014M 561211, and in part by the Fundamental Research Funds for the Central Universities under Grant K50511020032, Grant K5051302030, and Grant WRYB142105.

H. Yuan is with the North University of China, Taiyuan, Shanxi 030051, China, and also with the School of Electronic Engineering, Xidian University, Xi'an, Shaanxi 710071, China (e-mail: useryuanhaobo@163.com).

X. Dang and N. Wang are with the School of Electronic Engineering, Xidian University, Xi'an, Shaanxi 710071, China (e-mail: xjdang@mail.xidian.edu.cn; wangnan@mail.xidian.edu.cn).

Z. Wang is with the North University of China, Taiyuan, Shanxi 030051, China (e-mail: wzj@nuc.edu.cn).

Color versions of one or more of the figures in this communication are available online at http://ieeexplore.ieee.org.

Digital Object Identifier 10.1109/TAP.2015.2417897